A Fully-Integrated Self-Healing Power Amplifier

Steven M. Bowers, Kaushik Sengupta, Kaushik Dasgupta, and Ali Hajimiri

California Institute of Technology, Pasadena, California, 91125, USA

***Abstract* —A fully-integrated self-healing mm-wave power amplifier heals process variation, load mismatch, and transistor failure with on-chip sensors, actuators and an integrated digital algorithm ASIC without external calibration. Measurements of 20 chips showed increased RF power up to 3dB, or reduced DC power by 50% in backoff at 28 GHz. Healing 4-1 VSWR load mismatch for RF and DC power improvement was verified, and healing after laser induced transistor failure increased RF power up to 4.8dB.**

***Index Terms* — Actuators, CMOS Integrated Circuits, Digital Control, Power Amplifiers, Power Generation, Sensors, Thermal Sensors.**

I. Introduction

Silicon mm-wave integrated circuits have enabled numerous new high frequency applications that previously were not economically feasible. However, high power mm-wave design in nanometer scale CMOS technologies is particularly susceptible to transistor variations, model accuracy, environmental changes, and aging [1]. Reliable modeling is also a greater challenge in high frequency circuit design as the transistor parasitics contribute a larger fraction of the total relevant circuit capacitance. This is further exacerbated by the fact the models are often primarily optimized for digital circuits. Finally, aging effects and environmental variations such as load mismatch and temperature can significantly degrade the performance of mm-wave power amplifiers (PAs), where both output power and efficiency are strongly dependent on process and environmental parameters [2]. Self healing can mitigate these issues by identifying any degradation and modifying the parameters of the circuit to improve its performance post fabrication with minimum overhead [3,4]. In this work, integrated self healing of a PA is accomplished by using on-chip sensors, actuators, analog to digital converters (ADCs), digital to analog converters (DACs), and a digital application-specific integrated circuit (ASIC) providing a self-contained self-healing system.

This paper demonstrates a mm-wave PA system (Fig. 1) where on-chip self-healing improves the output power, gain, and DC power consumption under a broad range of non-idealities, such as process variations, modeling inaccuracies, load mismatch, and even catastrophic failure of amplifier. It is essential that the additional self-healing circuitry introduce minimal degradation of the RF performance with a low overhead in terms of area and power consumption. The individual actuator, sensor and data conversion blocks are presented in [5]. A sufficient actuation range is required to encompass the optimum state for all expected variations. Similarly, sensors robust to the very same variations they are trying to detect are also necessary and are achieved by using non-minimum length transistors and variation-insensitive topologies [5]. This allows for significant performance enhancements of the mm-wave system even when considering the associated costs of the self-healing circuitry.

This work was supported by the Air Force Research Laboratory. The views expressed are those of the authors and do not reflect the official policy of the Department of Defense or the U.S. Government.

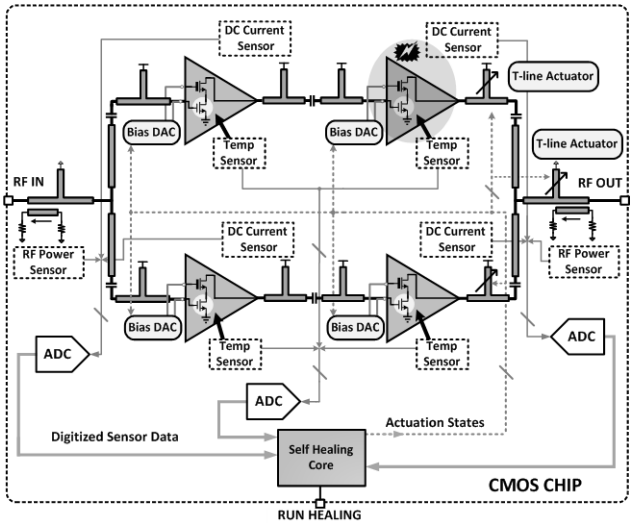

Fig. 1. Block diagram of self-healing power amplifier showing RF path, sensors, actuators, data converters and digital core.

II. Design

The self-healing power amplifier (Fig. 1) combines the power from two amplification stages using a 2:1 transmission-line-based output-combining network. Each amplifying path consists of two cascode stages, where thick gate-oxide common-gate transistors are used to improve gain and high voltage handling capability.

A. Actuators

The output matching network can be tuned though three tunable transmission line stub actuators (Fig. 2) that are programmed with digital switches that short the signal line to the local ground at various points [5]. This is especially useful for healing against load mismatches, as shown in the measurement plot of Figure 2, where the total output power of the PA was measured under two different load impedances while the actuator state of one of the transmission line stubs was swept. Additionally, gate voltages of the eight amplifier transistors are controlled independently by 6-bit low-power bias actuation DACs, enabling 5x actuation range of the DC power.

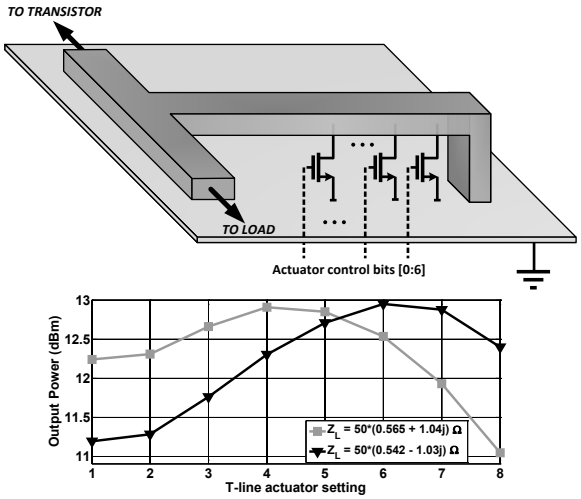

Fig. 2. Schematic of transmission line actuators and performance variation for different actuator states under different load mismatch.

B. Sensors and ADC

Low power, yet accurate sensors are essential to the self-healing system. The magnitudes of the input and output RF power are measured using two 20dB directional couplers with power detectors both at the coupled and isolated ports (Fig. 1). This facilitates detection of waves traveling both to the load and reflected from it, enabling accurate power sensing in the presence of load mismatch. The four supply voltage regulators associated with each amplification stage are modified to also serve as DC current sensors (Fig. 3). Junction temperature sensors utilizing interdigitated diodes between fingers of the amplifying transistors assess temperature differences between the transistor cores and other points on the chip, as a measure of the DC power consumption. On-chip 8-bit ADC's relay the sensor data to an integrated digital ASIC. Due to their robust design, no external calibration is needed or used in any actuator, sensor, DAC, or ADC [5].

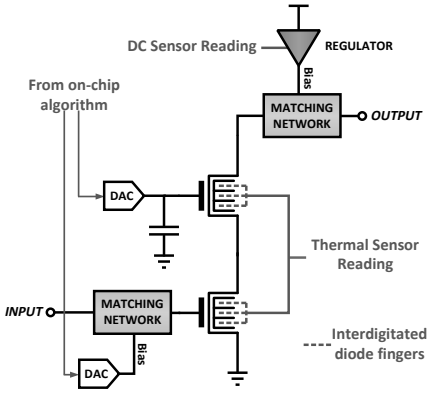

Fig. 3. Schematic of a single stage of the amplifier showing the DAC biasing, thermal sensor diodes, and voltage regulator with DC current sensor.

C. Digital Algorithm

The synthesized on-chip healing algorithm is made up of a global state machine that controls component blocks for actuation load, sensor read, and optimization. Because of this modular code setup, many different types of complex optimization algorithms can be incorporated into this general fully-integrated self-healing framework. Two such optimization strategies have been synthesized in the current implementation that finds the optimum solution within the search space of 262,144 possible states. One finds the state with maximum output power, and the other finds the state with the lowest DC power for a given output power. The convergence of the algorithm using a low frequency clock of 50MHz (limited by the measurement setup) takes up to a maximum of 0.8 seconds. At its full speed of 200 MHz, the maximum healing time would be 0.2 seconds.

III. Measurement

The self-healing PA system is fabricated in a 45nm SOI CMOS process and 20 chips were evaluated under nominal loads, 10 of which were also measured with mismatched load conditions generated by a variable mm-wave load tuner (Focus Microwaves 50GHz iTuner). Using simulations, actuator settings that maximize performance metrics of interest (e.g., output power) at saturation have been determined for typical transistors and are defined in measurements as "un-healed" default states. Because the default state was designed for saturation, it is closer to optimum than at lower input powers, and thus the healing is greater in back off conditions. After healing, the PA has a small signal gain of 21.5dB and a power added efficiency of 7.2% with output powers of 16dBm at saturation and 12.5dBm at the 1-dB compression point, while drawing 520mW of DC power at 28GHz.

Fig 4. shows output vs. input power in the default state as well as in the states healed at small signal and near compression. It shows that there is no one state that can provide the optimal performance at all input powers, but with self healing, the appropriate state for the current environment is automatically found. The two histograms in Fig. 4 show the improvement of 20 chips when healed in back-off and near compression.

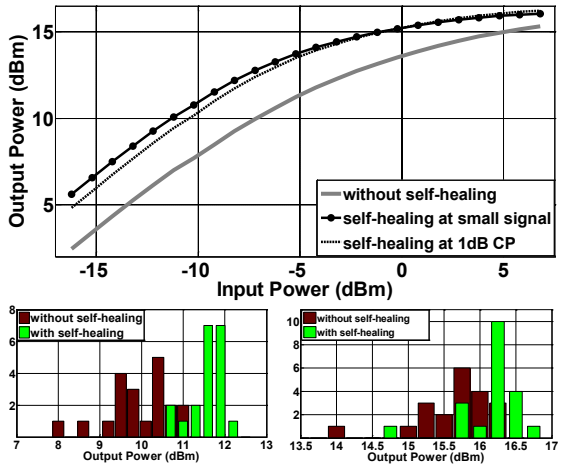

Fig. 4. Output power healing from default state to healed states at small signal and near compression with 20 chip histograms showing output power improvement in back-off and compression.

Using the on-chip algorithm to minimize DC power while maintaining a given output power, the DC power required to reach different output RF power levels with a minimum of 10dB gain is plotted for 20 chips and the cross section at Pout= 12.5dBm is shown as a histogram in Fig. 5.

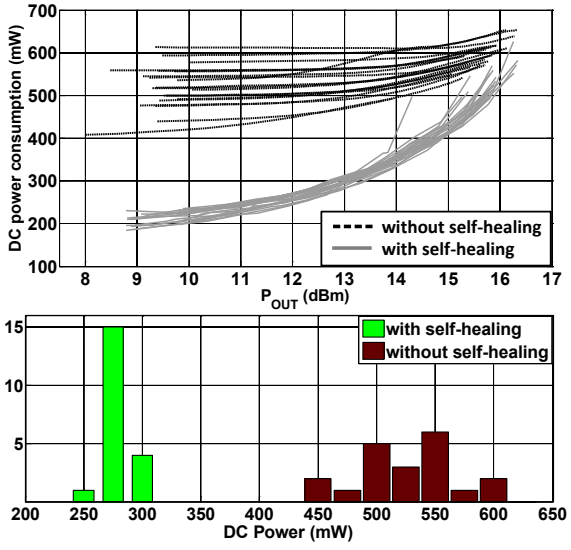

Fig. 5. DC power healing shown vs output power, with a 20 chip histogram showing variation at P_{out}=12.5dBm

Another critical benefit is that variation between chips is also significantly decreased with self healing, as seen in Fig. 5.

To demonstrate self healing under load mismatch, the on-chip algorithm is run for various VSWR points up to the 4:1 circle. Fig. 6a shows constant output power contours on a 50Ω Smith chart for 0.7dBm input power, under different load impedances using default settings as well as with self healing, showing dramatic improvement across all of the measured loads. The improvement across 10 chips for 2 specific load points is plotted as histograms in Fig. 6b.

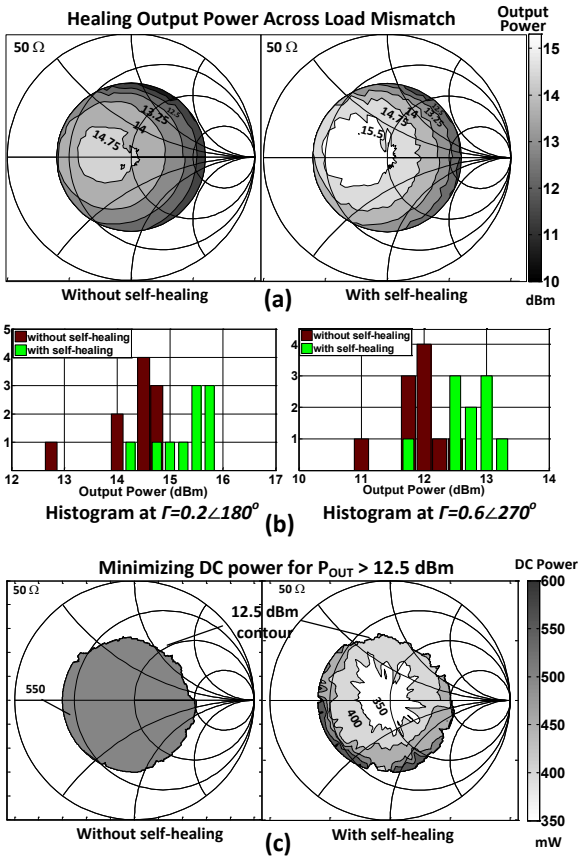

Fig. 6. a) Output power healing under load mismatch showing self-healing operation within the entire 4-1 VSWR circle. b) 10 chip histograms showing healing ability at 2 loads. c) DC power reduction while maintaining 12.5dBm output power.

One key advantage of this self-healing system is that it can provide a constant output power across VSWR events while simultaneously reducing the DC power consumption. To showcase this ability, the on-chip algorithm is instructed to keep 12.5dBm output power with minimum power consumption across all loads. As depicted in Fig. 6c, the healed PA is able to cut DC power levels by up to 33%.

The linearity of the PA is critical for applications involving non-constant envelope. Thus, the error vector magnitude (EVM) in both default and healed states were also measured under a 100ksps 16QAM modulation and a histogram of 10 chips for an output power of 12.5dBm is presented in Fig. 7. The improvement in linearity comes from the fact that with better matching, the same output power can be achieved at a lower level of transistor compression. This also highlights the ability of this system to operate as either a class A or class AB amplifier.

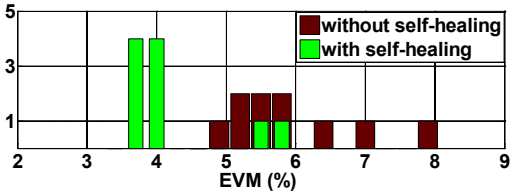

Fig. 7 EVM histogram for 10 chips at 12.5dBm output power and 100ksps 16QAM modulation before and after healing.

Finally, self healing was applied in the case of transistor failure by laser cutting parts of one of the two output amplifier stages (marked in Fig. 1). As shown in Fig. 8, measurements were taken after half of one of the common source transistors were cut out (8b), and then again after half of the cascode transistor was cut (8c). Finally, that entire amplifying stage was cut out (8d), dealing an 8 dB blow to the default state, that the on-chip healing algorithm was able to heal by up to 4.8dB, and 3.4dB at saturation, showing the utility of self healing particularly under extreme breakdown scenarios. As the default state goes further from optimum, the ability of the system to heal increases, even in saturation.

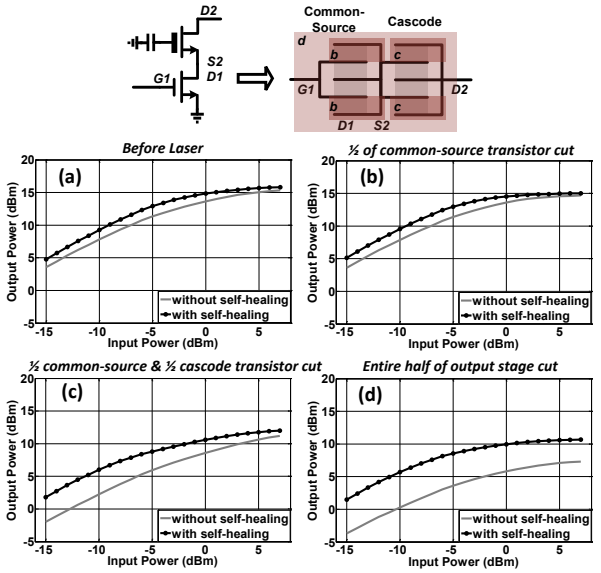

Fig. 8 Regions of laser cutting to create various levels of transistor failure, and output power vs. input power for default and after self healing.

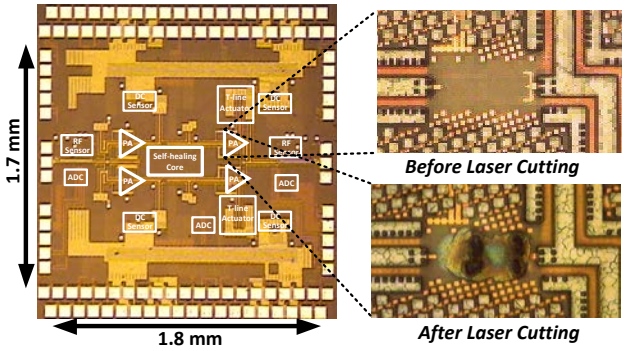

Fig. 9 Die photo of self-healing PA system showing RF blocks, sensors, actuators and self-healing digital core, and close up photos of output stage transistor before and after laser cutting.

VII. Conclusions

This paper demonstrates many of the substantial benefits and the flexibility provided by integrating a self-healing system with a mm-wave circuit such as a power amplifier. Two on-chip healing algorithms allow for significant increases in output RF power or decreases in DC power for a given output RF power. Healing against process variation and mismatch were verified with measurements from 20 chips, and healing load impedance mismatch and transistor failure was demonstrated.

Acknowledgement

The authors would like to thank Ben Parker of IBM for digital synthesis support.

References

[1] K. Bernstein, D.J. Frank, A.E. Gattiker, W Haensch, B.L. Ji, S.R. Nassif, E.J. Nowak, D.J. Pearson, and N.J. Rohrer, "High-performance CMOS variability in the 65-nm regime and beyond," *IBM Journal of Research and Development,* vol. 50, no. 4.5, pp. 433-449, Jul. 2006.

[2] A. Keerti and A.-V.H. Pham, "RF characterization of SiGe HBT power amplifiers under load mismatch," *IEEE Trans. Microwave Theory and Tech.*, vol. 55, no. 2, pp. 207-214, Feb. 2007.

[3] J.Y.-C. Liu, A. Tang, N.-Y. Wang, Q.J Gu, R. Berenguer, H.-H. Hsieh, W. Po-Yi, C. Jou, and M.-C.F Chang, "A V-band self-healing power amplifier with adaptive feedback bias control in 65 nm CMOS," *IEEE RFIC Symp.*, Jun. 2011.

[4] L. Sankey and Z. Popovic, "Adaptive tuning for handheld transmitters," *IEEE MTT-S Int. Microwave Symp. Dig.*, pp. 225-228, Jun. 2009.

[5] K. Sengupta, K. Dasgupta, S. Bowers, and A. Hajimiri, "On-Chip Sensing and Actuation Methods for Integrated Self-Healing mm-Wave CMOS Power Amplifier" *accepted, IEEE MTT-S Int. Microwave Symp.,* Jun. 2012.